Accelerated Neutral Atom Beam (ANAB) Technology for Nanoscale Surface Processing

S. Kirkpatrick*, M. Walsh**, J. Khoury* and D. Shashkov*
*Exogenesis Corp., Billerica, MA, USA, dshashkov@exogenesis.us
**Neutral Physics Corp., Albany, NY, USA

ABSTRACT

We use Accelerated Neutral Atom Beam (ANAB) technology to impart beneficial functionality on metal, ceramic, glass, and polymer surfaces without detrimental impacts of traditional plasma and ion beam technologies. ANAB provides an intense, collimated beam of energetic neutral gas atoms with highly controlled energies from 10-100eV per atom, an ideal range for many nanoscale surface modifications. We demonstrate ANAB impact in three distinct areas. The first is atomic-level smoothing and amorphization of the topmost few nm of material surfaces, resulting in better transmissive and reflective properties in a variety of optical applications. The second area is for improved adhesion of coatings, increasing laser-induced damage threshold (LIDT) and providing benefits for drug delivery applications, among others. Finally, we demonstrate the use of ANAB for creation and modification of thin films and nano-membranes, with benefits to such diverse fields as EUV lithography, low-energy electron microscopy, and nano-filtration.

Keywords: super-polishing, laser-induced damage threshold, oxidation resistance, coating adhesion, amorphization

1 BACKGROUND

It has long been recognized that nano-scale modifications of solid surfaces and thin films can result in improved performance of devices ranging from semiconductor structures to optical elements and medical implants. However, existing surface modification technologies fall short of the nano-scale requirements for such modifications due to high particle energy and electrically charged nature of traditional ion beams and plasma-based techniques. An ideal surface treatment would employ electrically neutral species and have controllable energies capable of exceeding the sputtering thresholds of target materials while not introducing long-range sub-surface damage characteristic to high-energy particles.

2 ANAB TECHNOLOGY

The Accelerated Neutral Atom Beam (ANAB) is a novel particle beam technology that provides the right combination of particle type and energy for highly controllable material modification or removal from the surface at the nanoscale, without damaging the underlying bulk material. As previously described [1], with ANAB, a stream of clusters is formed via adiabatic expansion of pressurized gas into vacuum through a specially shaped nozzle. Clusters of 500-5,000 atoms (approximately spherical in shape, 1-4 nm diameter) are formed, bound by van der Waals forces. The clusters are then ionized by electron impact ionization and accelerated to energies from 20-50 kV. Cluster dissociation is then promoted by orchestrating cluster collisions with slow-moving gas molecules present along the flight path. Finally, all charged species are removed from the beam by an electrostatic deflector. The resulting beam contains accelerated neutral atoms with controllable energies from ~10 eV to ~100eV. With ANAB, the dissociated clusters form "clouds" of individual gas atoms or molecules traveling in close proximity to each other with essentially the same speed and direction and arriving nearly simultaneously to the target surface.

3 SURFACE SMOOTHING AND AMORPHIZATION

Angstrom-level touchless smoothing of various optical (reflective and transmissive) surfaces using ANAB has been demonstrated [2, 3]. Reduction in average (Ra) and peak-to-peak (Rz) surface roughness relies on lateral sputtering property of ANAB. Figure 1 illustrates ANAB smoothing of an Extreme Ultraviolet (EUV) lithography mask blank substrate, as measured by Atomic Force Microscopy (AFM).

Similar improvements in roughness have been observed for a variety of crystalline and amorphous optical materials, summarized in Table 1.

Material	Initial Ra (nm)	Final Ra (nm)
Spinel ($MgAl_2O_4$)	2.81	0.71
Ge	0.98	0.68
ZnS	1.78	0.65
Aluminum	5.67	0.60
SiC	1.98	0.40
Fused silica (low quality)	0.62	0.36
Polycrystalline diamond	0.50	0.21
MgF_2	1.29	0.20
CaF_2	0.48	0.17
Fused silica (high quality)	0.34	0.17
LBO	0.96	0.15
Yb:YAG	0.31	0.15
EUV mask blank	1.22	0.13
Quartz	1.22	0.13
Sapphire	1.40	0.11

Table 1: Average roughness achieved by ANAB smoothing.

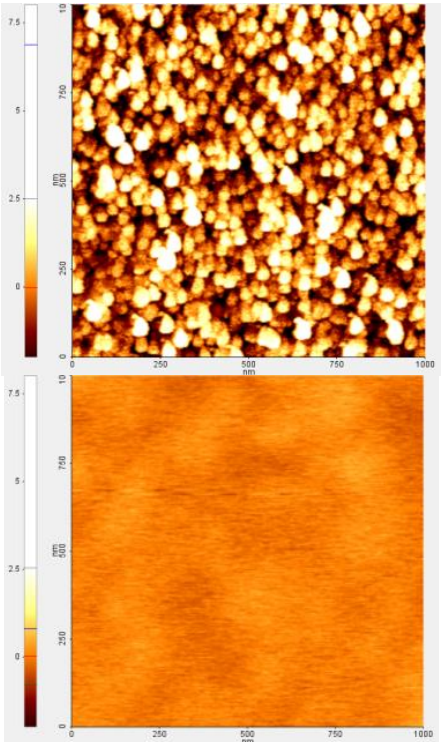

Figure 1: AFM image of EUV mass blank substrate (Ti-doped silica glass), 1μm^2 scan area in non-contact mode. (Top) Untreated substrate: R_a = 1.22 nm, R_z = 11.2 nm (Bottom) ANAB-treated substrate: R_a = 0.13 nm, R_z = 1.41 nm.

In addition to smoothing, ANAB also creates a thin (2-3 nm) amorphous layer on crystalline surfaces, where its thickness depends on beam energy and the type of material. Figure 2 is a cross-sectional TEM (XTEM) image of an amorphous region formed on [100] Si surface by 30 kV Ar-based ANAB. Notably, the thickness of this amorphous layer is only 2.1 nm, while the interface between the crystalline and amorphous regions of the irradiated silicon remain atomically smooth.

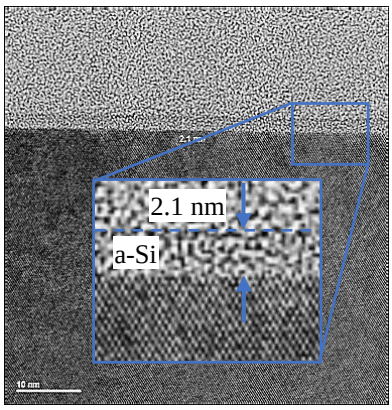

Figure 2: XTEM of an atomically-flat amorphous layer formed by ANAB irradiation of a [100] Si surface

Amorphous surface layers may also protect against atmospheric degradation. We demonstrate this by ANAB treatment of a polycrystalline Cu film and subsequent oxidation at 200C in atmosphere for 2 min. Fig. 3 shows a comparison between the ANAB-treated and untreated regions of the film, clearly indicating oxidation of the untreated film, while the ANAB treated region retained the color of unoxidized copper. We hypothesize that formation of an amorphous layer via ANAB irradiation creates a thin but highly effective barrier against oxygen grain-boundary diffusion into the film, a dominant oxidation mechanism at such low temperature. We are currently investigating similar protective mechanism on sputtered Cr thin films widely used as reflective surfaces for X-ray mirrors.

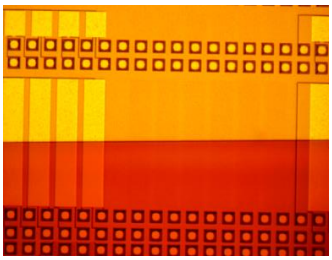

Figure 3: ANAB treatment of Cu film (top half) results in passivation against atmospheric oxidation at 200C for 2 min, as compared to untreated film (bottom half).

The surface smoothing abilities of ANAB have already been proven useful for significantly increasing the Laser-Induced Damage Threshold (LIDT) of laser optics [2-4]. These results are summarized in Table 2.

Material	**LIDT (untreated), J/cm^2**	**LIDT (ANAB treated), J/cm^2**	**Relative increase**
CaF_2	50	70	40%
Yb:YAG	10.4 (back surface) 9.5 (front surface)	16.2 18.2	56% 92%
LBO	50	120	140%

Table 2: ANAB impact on Laser Induced Damage Threshold (LIDT) of various optical materials.

Evaluation of LBO surface after LIDT measurement revealed a difference in damage pattern, as illustrated in Figure 4. The untreated crystal has a typical spray pattern, while ANAB-treated crystal shows an uncharacteristic symmetric pattern. This difference in failure modes warrants further investigation.

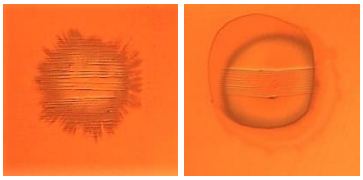

Figure 4: LBO surface after laser damage testing; untreated crystal (left) and ANAB-treated crystal (right).

Based on the above results, we view ANAB as the premier technique in achieving angstrom-level smoothing of optical surfaces while minimizing subsurface damage. Combined with the ability to form protective layers on metal surfaces, ANAB can prove an indispensable tool in optimizing laser optics [4], X-ray and neutron mirrors [5], and other demanding optics and photonics applications.

4 COATING ADHESION

In addition to surface smoothing, ANAB has been shown to improve coating adhesion. This improvement stems from increases in surface area and surface energy. This is a result of nano-textures created on various surfaces under certain conditions, and the direct outcome of surface amorphization and the formation of dangling bonds on the target surface, as has been demonstrated by contact angle measurements [6] and surface chemistry analysis [7].

Similar to uncoated laser optics, ANAB treatment has been shown to increase LIDT of Yb:YAG crystals with SiO_2/Ta_2O_5 anti-reflective (A/R) coatings [4]. Specifically, ANAB-textured surfaces have demonstrated the largest increase in LIDT, supporting the hypothesis that the increased surface area of a nano-textured surface contributes to increased coating adhesion.

In a different application, ANAB was shown to increase polyetheretherketone (PEEK) polymer adhesion to epoxy. The experiment is illustrated in Figure 5. In a standard ASTM F1147 setup commonly used to measure coating adhesion under uniaxial tensile load, the PEEK sample was attached to stainless steel using green epoxy as an adhesive. As expected, untreated PEEK separated from the epoxy upon fracture, reflecting relatively low adhesion strength. In the case of ANAB-treated PEEK, we observed the fracture plane forming through the bulk of the adhesive, illustrating significant increase of PEEK/epoxy interfacial strength as a result of ANAB treatment.

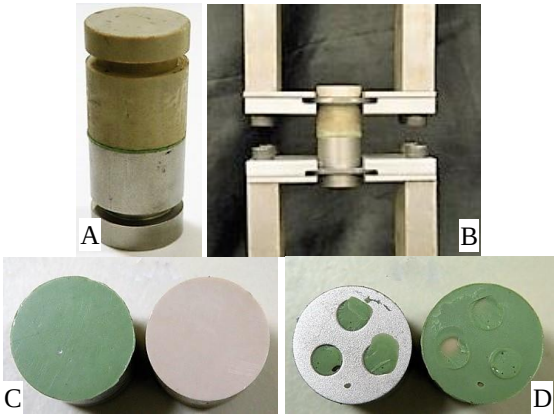

Figure 5: Improved PEEK/epoxy adhesion after ANAB treatment. (A) PEEK/epoxy/stainless steel specimen; (B) uniaxial tensile testing setup; (C) untreated PEEK sample fractured at PEEK/epoxy interface; (D) ANAB treated PEEK specimen fractured through epoxy film.

In another example, we have used a simple tape test to measure adhesion of a drug coating to silicon. Two silicon wafers were either ANAB-treated or untreated and spray coated in vacuum with rapamycin, a common anti-stenosis drug and an immunosuppressant. Upon drying of the coating, adhesive tape was applied to the coating and removed after 1 minute. Figure 6 illustrates the differences between untreated and ANAB-treated Si substrates. As in prior examples, ANAB treatment increased coating adhesion.

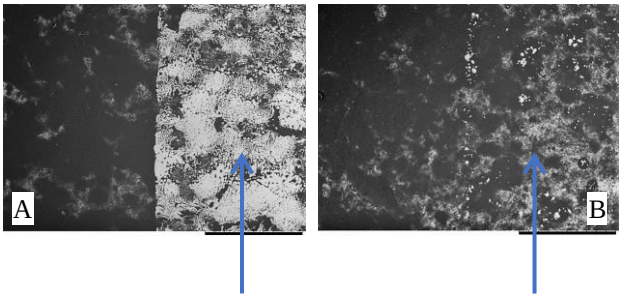

Figure 6: Improved rapamycin coating adhesion to Si after ANAB treatment. Drug coating appears dark in SEM. Arrows indicate the area of tape application. Scale bar: 1 mm. (A) untreated Si; (B) ANAB-treated Si.

The three examples above illustrate a broad range of coatings (ceramic, polymer, and organic drug molecules) applied by different techniques. In all cases, ANAB treatment of the underlying substrate substantially improves coating adhesion, making the technique a strong candidate to bring about improved laser optics, polymer coatings, and drug delivery.

5 THIN FILM FORMATION AND MODIFICATION

Our final set of examples relates to creation and modification of free-standing thin films. Due to the low energy range of ANAB, its extremely shallow sub-surface impact, and its neutral nature, it is capable of modifying thin and ultra-fragile materials without damage. We have utilized ANAB to reduce the thickness of Si nitride (Si_3N_4) EUV pellicle material from 200 nm to 80 nm (Figure 7). As a result, its EUV transparency increased from 25% to 85%, addressing a persistent challenge for EUV pellicle creation.

As a second example, we demonstrate ANAB capability in creating and handling a film with thickness of just a few nanometers. An amorphous carbon film 2.5 nm thick has been created via irradiation and reduction of a thin polymer film with ANAB and subsequent chemical removal of the un-reduced polymer layer (Figure 8) forming a continuous thin membrane TEM grid for ultra-low energy microscopy. At such low thickness, its measured electron transparency meets or exceeds that of graphene and provides complete open span coverage without wrinkles and voids.

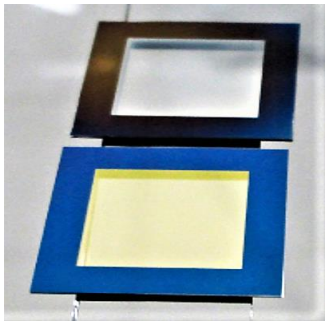

Figure 7: Thinning of Si nitride EUV pellicle. Bottom: as manufactured; thickness = 200 nm, EUV transparency = 25%. Top: ANAB-etched membrane thickness = 80 nm, EUV transparency = 85%.

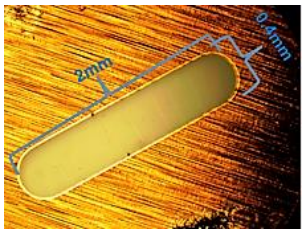

Figure 8: 2.5 nm thick free-standing, continuous amorphous carbon film formed by ANAB across a macroscopic area.

Another method to create such thin free-standing carbon films is by utilizing carbon-containing ANAB gases such as methane. Under certain conditions, a nanometer-thick carbon scaffold is left on the irradiated specimen surface. This scaffold can then be turned into a free-standing film by dissolving the substrate. This technique was used to create and characterize amorphous carbon films shown in high-resolution TEM in Figure 9. The film is extremely dense and uniform at approximately 2 nm thickness across a macroscopic area (100 μm TEM grid) [8].

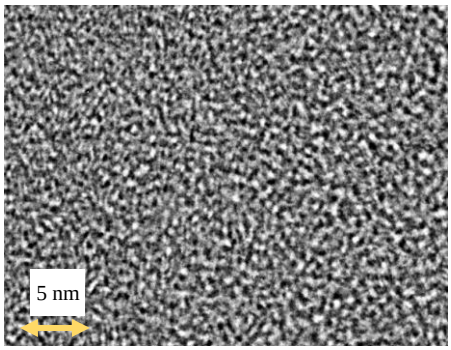

Figure 9: TEM of free-standing 2 nm amorphous carbon film formed by carbon-containing ANAB exposure.

Finally, we utilized Gas Cluster Ion Beam (GCIB) technology, a predicate to ANAB, to irradiate membranes of graphene and graphene oxide (GO) [9] to create nano-porous membranes. Figure 10 shows an AFM image of GO with multiple holes perforated by GCIB, ranging in size from 5 nm to 14 nm, averaging 8 nm. Nano-porous membranes are finding numerous applications in the fields of water desalination, chemical separation, and DNA research.

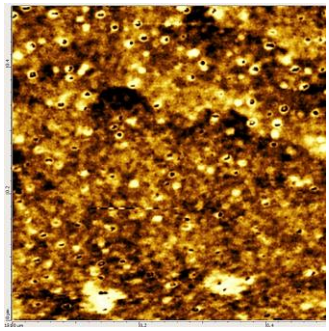

Figure 10: Nano-pores of 8 nm average diameter formed in GO by GCIB irradiation. Field of view: 500 nm x 500 nm.

6 CONCLUSIONS

ANAB technology offers highly controllable surface modification capability at the nanoscale. It can be used to controllably remove material, amorphize and smooth optical surfaces to an angstrom level, improve coating adhesion, as well as create and modify nanometer-thick free-standing films. These enabling capabilities are finding increasing utility in diverse fields of use ranging from optics to electronics to biomedical research.

REFERENCES

[1] A. Kirkpatrick, S. Kirkpatrick, M. Walsh, S. Chau, M. Mack, S. Harrison, R. Svrluga and J. Khoury, Nuclear Instr. and Methods in Phys. Res. B, **307**, 281-289, 2013.

[2] M. Walsh, K. Chau, S. Kirkpatrick, R. Svrluga, Proc. SPIE **9237**, 2014, 92372I.

[3] S. Kirkpatrick, M. Walsh, R. Svrluga, M. Thomas, Proc. SPIE **9632**, 2015, 96321Y.

[4] M. De Vido, M. Walsh, S. Kirkpatrick, R. Svrluga, K. Ertel, P. Phillips, P. Mason, S. Banerjee, J. Smith, T. Butcher, C. Edwards, C. Hernandez-Gomez, J. Collier, Opt. Mater. Express **7**(9), 3303-3311 (2017).

[5] "Atomically smooth surfaces as substrates for advanced neutron supermirrors", SBIR award, https://www.sbir.gov/sbirsearch/detail/1504931.

[6] J. Khoury, S. Kirkpatrick, M. Maxwell, R. Cherian, A. Kirkpatrick, R. Svrluga, Nuclear Instr. and Methods in Phys. Res. B, **307**, 630-634, 2013.

[7] Khoury J, Maxwell M, Cherian RE, Bachand J, Kurz AC, Walsh M, Assad M, Svrluga RC, J. Biomed. Mater. Res. B, **105B**, 531-543, 2017.

[8] Image courtesy of Norcada Inc.

[9] Image courtesy of Prof. Z. Insepov (Purdue Univ.).